SIMULATION OF STRONG MOTIONS USING PARAMETERS BASED ON RECORDED ACCELEROGRAMS

Sanshiro SUZUKI[1] And Koichiro ASANO[2]

SUMMARY

It is generally difficult to predict with certain accuracy when and where a big earthquake will take place. We need to take into account the strong effect of severe ground motions of shear wave on the dynamic behavior of buildings and civil structures. We simulate strong motions of pure shear wave and synthesize small motions, using the recorded accelerograms at a site on a base rock in northern Osaka, Japan. By making use of a stochastic technique, we can easily introduce higher frequency contents in the motions and apply the technique to the synthesis of small waves that are regarded as green functions. We also introduce to the analysis the useful relationships among the seismic moment M_0 and the time duration T_d, M_0 and the corner frequency f_c, and M_0 and the high cutoff frequency $f_{\max}$, which were regressed by a simple representation scheme. We demonstrate analytical and recorded accelerograms and their spectra, and compare all of them. We show the synthesis accelerogram of the respective waves that generate from small fault elements and try to predict strong ground motions, by considering active faults that will affect severe damage on almost structures in the Osaka basin.

INTRODUCTION

Recorded strong accelerograms of earthquakes have been chosen as input excitations for an aseismic design for high rise buildings. However, it is noticed that the recorded accelerograms have their own different characteristics wherever an earthquake takes place. There are mainly three reasons for this fact, that is, 1) source characteristics of earthquake, 2) path characteristics of seismic wave, and 3) soil characteristics around any site.

In order to simulate strong ground motions, the corresponding parameters for modeling are determined for the source, the path and the soil. The parameters of deep soil structure are not made clear at all desired sites. Under these conditions, the following three technique have been considered as to the simulation of strong ground motions: 1) the technique for the wave simulation of large earthquake based on assuming small earthquake waves as a green function (Irikura 1986), 2) the numerical technique (Lam 1904), and 3) the stochastic technique (Boore 1983). Each technique has its merits and demerits. From the seismic engineering viewpoint, the simulations of strong ground motions with higher frequency contents are desired and therefore, a technique that has the advantage of the theory and the experiment should have been developed.

In this paper, we refer the above first and third techniques, by which we can easily estimate higher frequency contents into the simulation, use the recorded accelerogram without the detail site conditions, and obtain strong ground motions with the stochastic characteristics. The parameters used for the simulation were chosen from regressive analysis among parameters based on 25 recorded accelerograms of earthquakes at an observation point, where is almost regarded as base rock at the Takatsuki campus of Kansai University in northern Osaka, Japan. We first compare the recorded accelerograms and the analytical ones and their spectra, and then show the synthesis accelerogram of the respective waves that generate from small fault elements.

[1] *Faculty of Engineering, Kansai University, Osaka, Japan. Email; sanshiro@ipcku.kansai-u.ac.jp*
[2] *Faculty of Engineering, Kansai University, Osaka, Japan. Email; asano@ipcku.kansai-u.ac.jp*

METHODOLOGY

Stochastic simulation

Referring to the description of Boore's paper, which considered a point source, the acceleration spectrum $A(f)$ of shear waves at a distance r from a fault with seismic moment M_0 is

$$A(f) = CM_0 S(f, f_c) P(f, f_{\max}) r^{-1} \exp(-\pi f r / Q\beta), \tag{1}$$

in which C is a constant given by

$$C = R_{\theta\phi} FS \cdot PRTITN / (4\pi\rho\beta^3). \tag{2}$$

$R_{\theta\phi}$ is the radiation pattern, FS is the amplification due to the free surface, $PRTITN$ is the reduction factor, and Q, ρ and β are the Q-value, the density and the shear wave velocity. The source spectrum S is given by the $\omega-$square model and used in the analysis as follows (Aki 1967, Brune 1970):

$$S(f, f_c) = (2\pi f)^2 / \left\{1 + (f / f_c)^2\right\}, \tag{3}$$

in which f_c is the corner frequency. $P(f, f_{\max})$ in equation (1) is a high-cut filter and expressed by the following function,

$$P(f, f_{\max}) = \left\{1 + (f / f_{\max})^{2s}\right\}^{-\frac{1}{2}}, \tag{4}$$

in which s controls the decay rate of higher frequencies above some high-frequency cutoff $f_{\max}$ and it was determined by recorded acceleration spectra.
We define an effective time duration T_d such as 5% to 90% of accumulation power for the shear wave motions of 25 recorded accelerograms of earthquakes can be estimated (Trifunac 1975). The JMA magnitude M_{JMA} of the earthquakes was between 3.5 and 5.5 except the case of the Hyogo-ken Nanbu earthquake, 1995. An experiment envelope function $w(t)$ of accelerogram is given by

$$w(t) = at^b \mathrm{e}^{-ct} H(t) \tag{5}$$
$$: a = (e / \varepsilon T_d)^b, \quad b = -\varepsilon \ln(\eta) / \left[1 + \varepsilon\left\{\ln(\varepsilon) - 1\right\}\right], \text{ and } \quad c = b / \varepsilon T_d,$$

in which $H(t)$ is the unit-step function, and ε and η are the parameters to prescribe the envelope function.

Synthesis simulation

Referring to the description of Irikura's paper, we also consider a rectangular fault plane, of which size is the length L and the width W, to simulate strong ground motions considering near field source. The plane has $l \times m$ elements of which size should be taken to match the fault plane size. The last synthesis expression form for target earthquake U is as follows using the waves u generated from the element:

$$U(t) = \sum_{i=1}^{l}\sum_{j=1}^{m} \frac{F_{ij}^s}{F_0^s} \frac{r_0}{r_{ij}} u(t - t_\xi) + \sum_{i=1}^{l}\sum_{j=1}^{m}\sum_{k=1}^{(n-1)n'} \frac{F_{ij}^s}{F_0^s} \frac{r_0}{r_{ij}} \frac{1}{n'} u\left(t - t_\xi - \frac{(k-1)\tau}{nn'}\right). \tag{6}$$

In which F is the radiation pattern (Aki & Richard 1980), τ the rise time, r the distance, n' the coefficient of subdividing, and $t_\xi = (r_{ij} - r) / \beta - \xi_{ij} / v_r$. ξ_{ij} is the distance between the rapture starting point and the element (i, j) and v_r is the rapture velocity.

REGRESSION

First of all, we drew the parts of shear wave from 25 recorded accelerograms and used them as the strong ground motions. The effective time duration T_d of them expressed in equation (5) was regressed as a function of the magnitude M_{JMA} and the distance r as follows:

$$\log(T_d) = 0.18M_{JMA} + 0.54\log(r) - 0.86 . \qquad (7)$$

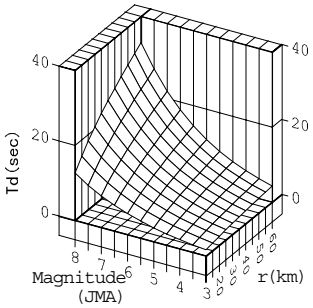

Figure 1. Relation among effective time duration, magnitude and epicentral distance.

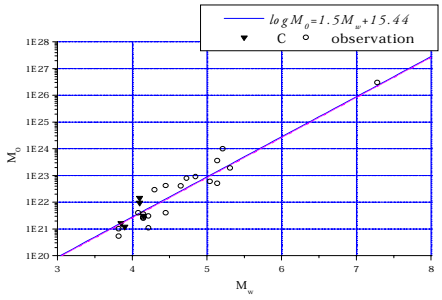

Figure 2. Relation between moment magnitude and seismic moment.

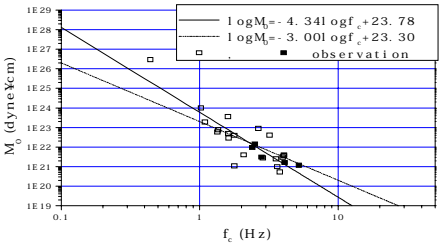

Figure 3. Relation between moment magnitude and corner frequency

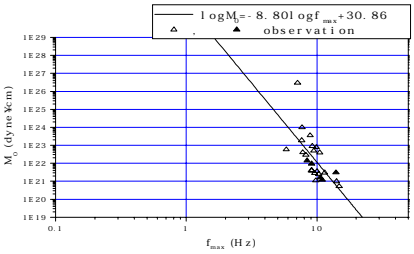

Figure 4. Relation between moment magnitude and high cutoff frequency.

The relation of equation (7) is shown in Figure 1. From the figure, it is noticed that T_d has long time duration for the larger magnitude and the longer distance.

It is considered to be more reasonable to use the seismic moment M_0 than the JMA magnitude M_{JMA} and the moment magnitude M_w. Therefore, we used the relation among the magnitude scales (Utsu 1982) and obtained M_w from M_{JMA}. Figure 2 shows the relations between M_0 and M_w by the square dots. As a result, we got the regressive relation between the two moments as follows:

$$\log(M_0) = 1.5M_w + 15.44 . \qquad (8)$$

It is seen from Figure 2 that the regression having the coefficient 1.5 is very good agreement with the observation data.

The spectral shape given by the $\omega-$square model depends on M_0, the corner frequency f_c and the high-frequency cutoff $f_{\max}$. We regressed two relations between M_0 and f_c, and M_0 and $f_{\max}$ based on the spectra. The respective relations between M_0 and f_c, and M_0 and $f_{\max}$ are able to be regressed directly from the recorded accelerogram spectra. They are respectively shown in Figures 3 and 4, in which the symbols represent the results for the 25 recorded accelerograms. The relation of M_0 and f_c leads to the following regression functions.

$$\log(M_0) = -3.00\log(f_c) + 23.30 \qquad (9a)$$

$$\log(M_0) = -4.42\log(f_c) + 23.78 \qquad (9b)$$

Equation (9a) is the regression function with the slope of –3.00 and equation (9b) is faithful to the original data in regression. There is some difference between the two functions. The relation of M_0 and $f_{\max}$ relation leads to the following regression functions.

$$\log(M_0) = -8.80\log(f_{\max}) + 30.86 \tag{10}$$

It is seen from Figure 4 that the value of $f_{\max}$ is about 10.0 *Hz* and the maximum is almost 16 *Hz*.

RESULTS

Stochastic simulation

As mentioned above, we can calculate the average accelerograms of the shear wave in the frequency domain using the amplitudes and phase characteristics of the Gaussian white noise, the distance from the source to the observation point, the soil damping *Q*-value depending on the frequency (Fukushima & Midorikawa 1994). The other parameters are ρ=2.7t/m^3, β=3.6km/sec, $R_{\theta\phi}$=0.63, FS=2.0, $PRTITN$=0.71, ε=0.16, η=0.21 in equations (1) to (5), referring to the Boore's paper. The accelerograms in the frequency domain thus obtained can be transformed to those in the time domain. The simulated accelerograms obtained are compared with the corresponding recorded ones at the Takatsuki campus of Kansai University for two different earthquakes. Figure 5 is the result in case of a moderate earthquake of M_w=4.3 ($r = 40$ Km), and (a) and (b) in the figure respectively represent the simulated and recorded accelerograms. Both maximum accelerations of 1.16 and 1.01 cm/sec^2 are very close with each other. The time duration T_d of the shear wave is approximately 5.0 sec, and the envelope function of the simulation is similar to the record. This means that the envelope function for moderate earthquakes can be regressed based on almost the recorded accelerograms.

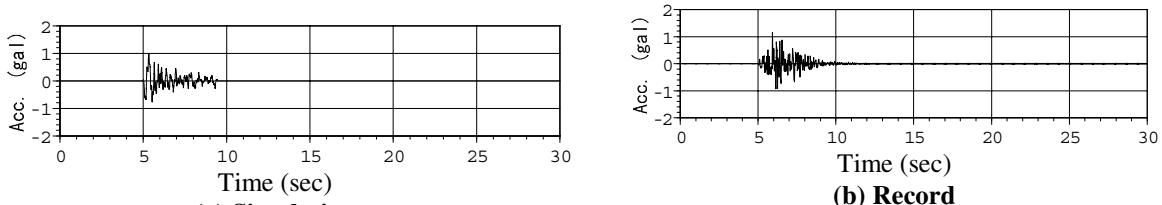

(a) Simulation **(b) Record**

Figure 5. Recorded and simulated accelerograms for a moderate earthquake, M_w=4.3, r=40 Km.

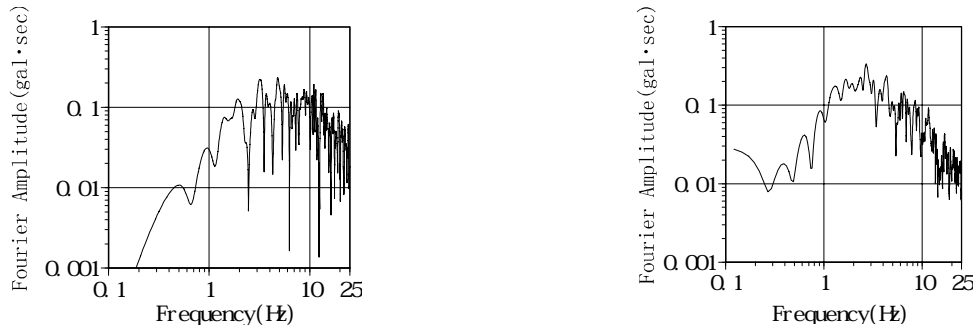

(a) Simulation **(b) Record**

Figure 6. Recorded and simulated spectra for a moderate earthquake.

Figure 6 is the Fourier spectrum obtained from Figure 5. The spectrum (b) corresponding to the moderate earthquake record is a little bit of different from the $\omega-$square model in the lower frequency domain, while the spectrum (a) corresponding to the simulation has good agreement with the $\omega-$square model. However, it can be found that this difference has no influence on the time history of acceleration as shown in figure 5. The frequency contents of the simulated accelerogram seem to be similar to the recorded one.

Table 1 shows the parameters of the moment magnitude, the fault plane size and the epicentral distance for three point sources and one point source as a whole of them for the Hyogo-ken Nanbu earthquake (Kikuchi, 1995).

Table 1: Point source parameters

Event No.	Moment Mw	Fault Plane $L*W$ (Km^2)	Distance r (Km)
1	6.8	24*12	52.7
2	6.3	9*5	42.8
3	6.4	12*6	41.0
Whole*	6.9	40*10	52.7

* Whole represents the summation of three events.

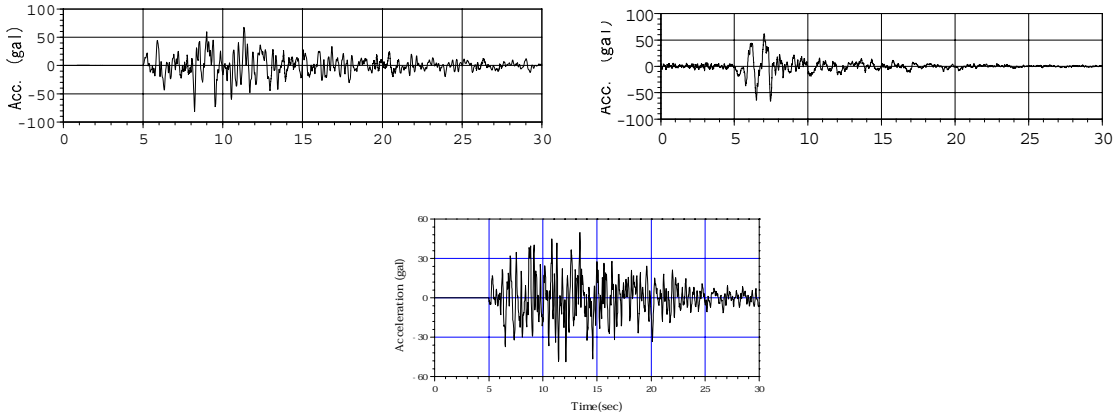

Figure 8. Simulated accelerogram for the Hyogo-ken Nanbu earthquake in case of three events.

Figure 7 (a) and (b) respectively show the simulated and recorded accelerograms of the horizontal component. The maximum value of the simulation is a slight larger than the one of the record. This is mainly because the source spectra were obtained by the regression of many moderate earthquake data assumed as a point source. As mentioned before, this result shows that T_d for a larger earthquake has longer time duration (see Fig. 2). Therefore, the recorded accelerogram near the source for a large earthquake do not have a good agreement with the simulated one. This is because the average values on the associated various parameters were used and the source was assumed to be a point far from the observation point.

Figure 8 shows the horizontal accelerogram obtained by the three points as a source model. Three accelerograms for each event are synthesized in the time domain. From this figure, it is found that the high frequency components are included in the time history compared with Figure 7 (a) and confirmed by the Fourier spectrum. A little bit of modification, in which the variation of the parameters is introduced, will gain better results. We need consider a near source model and source parameters to simulate and to predict strong ground motions.

Synthesis simulation

Referring the Hyogo-ken Nanbu earthquake, we use the parameters of the "Whole" of the single fault shown in Table 1. Each element size of the fault should be taken to match the fault size. We chose the coefficients of fault dividing to $l = m = n = 5$ and $r_0 = 1.0$ Km, and assume the starting point of rapture to the south-bottom element. The seismic moment is $M_0 = 2.5 \times 10^{26}$ (dyne$\times$cm).

Table 2 shows the parameters of the strike, the dip and the slip angles on the fault plane and the depth to the top of the fault. The reasons why we chose the dip and slip angles to 90 degrees are that this paper is the first step of the synthesis simulation and that we obtain the steady and fundamental data on the accelerogram of strong ground motion for prediction. Therefore, it is noted that the various parameters of the analytical fault model are differing from the fault of the Hyogo-ken Nanbu earthquake.

Table 2: Fault parameters

Strike angle ϕ(°)	Dip angle δ(°)	Slip angle λ(°)	Depth (Km)
233	90	90	10

Table 3: Soil parameters and characteristics of site

Stratum	α (Km/sec)	β (Km/sec)	ρ (t/m^3)	Q_p	Q_s	Thickness (Km)
1	4.9	1.2	2.2	800	250	1.0
2	5.3	2.7	2.7	1000	300	∞

The soil structure around the Takatsu campus is assumed to be the two-stratum structure, and the soil parameters and characteristics of it are shown in Table 3. In the table, α and β are respectively the $P-$ and $S-$wave velocities and Q_p and Q_s are the corresponding Q values.

Figure 9 shows the NS component of synthesized accelerogram. The time duration of strong motion is about 5 seconds and longer than the one of the record of the Hyogo-ken Nanbu earthquake (see Figure 7 (b)). The peak value of acceleration is around 100 cm/sec^2 and larger than the one of record. It is clear that more high frequency contents are included in the accelerogram compared with the other results shown in Figures 7 (a) and 8 (a) and that the whole time duration is roughly harmony with the record.

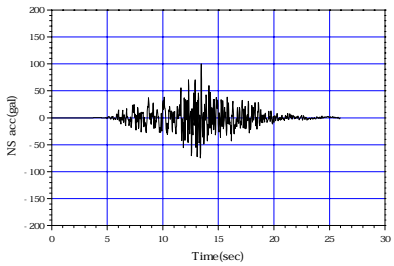

Figure 9. NS component of synthesized accelerogram.

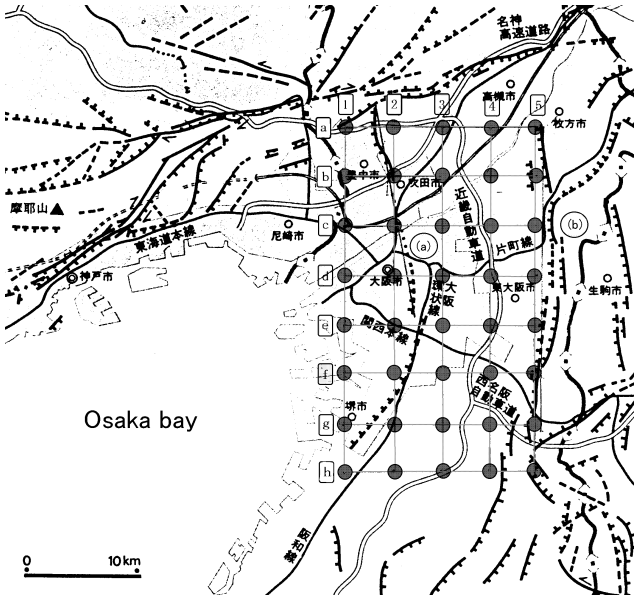

Figure 10. 40 observation points (black circle) in the Osaka basin and two active faults: (a) Uemachi and (b) Ikoma.

Table 4: The fault parameters of Uemachi and Ikoma models.

Fault	Fault plane $L*W$ (km^2)	Strike ϕ(°)	Dip δ(°)	Slip λ(°)	M_0 (dyne*cm)	Slip D (cm)	Rise time τ (sec)
Uemachi	20*24	350.5	90	90	$1.44*10^{26}$	88	90
Ikoma	28*24	360.0	90	90	$1.89*10^{26}$	83	90

Figure 10 shows the 40 observation points in the Osaka basin with black circle, in which the distance between two points is 5 Km. We choose two active fault models in the basin, of which names are Uemachi and Ikoma, to simulate strong ground motions at the 40 points. The fault models are respectively designated by (a) and (b) in the figure. The fault (a) is located in the center of the Osaka city and (b) in the eastern edge of the basin. The parameters of the length L, the width W, the strike, the dip and the slip angles (respectively, designated by ϕ, δ and λ), the seismic moment M_0, the slip D and the rise time τ are listed for the two faults in Table 4 (Somervill et al. 1993).

Attenuation of maximum acceleration

Figure 11 (a) shows the maximum acceleration values of the two horizontal components as a function of the distance r for the 40 observation points in case of the Uemachi fault model without the surface layer thickness on the fault, d =0.0. In the figure, two attenuation curves can be seen. The attenuation curve (1) is illustrated based on the attenuation curve (Fukushima et al. 1994) and the curve (2) is modified to reduce at the far distance for near source strong motions. Figure 11 (b) is the result in case of the Uemachi fault model with the surface layer thickness, d =1.0 Km. The similar attenuation curves (1) and (2) are also illustrated in the figure. The maximum acceleration values of the figure (a) do not agree with the attenuation curves because of the large variation of acceleration value. From the figure (a), the maximum accelerations are harmony with the attenuation curves compared with the figure (b). In particular, the modified curve has a good agreement with the acceleration values for the distance.

Figure 12 (a) and (b) are the results of the maximum acceleration values for the two horizontal components as a function of the distance r for the 40 observation points in case of the Ikoma fault model with d =0.0 and d =1.0 Km, respectively. In these figures, two attenuation curves can be also seen. The maximum accelerations in case of d =0.0 are less estimation than the attenuation curves. On the other hand, In the case of d =1.0, those are larger estimation than the attenuation curves. The surface layer on a fault will affect the maximum acceleration of strong ground motions. When we assume a near source and simulate strong ground motions for the prediction, it will be difficult to determine the definition of the exact distance from the source to an arbitrary observation point and therefore, we should be careful of the use of attenuation curves.

CONCLUSIONS

The relationships among the seismic moment M_0, the corner frequency f_c and the high cutoff frequency $f_{\max}$ were regressed by a simple representation scheme and used to simulate horizontal strong ground motions of shear waves including average characteristics of the source, the path and the site at the observation point. The simulated accelerograms reproduced the recorded ones with an engineering sufficiency on their maximum values and the effective time duration T_d based on the recorded accelerograms.

In particular, the simulation wave with higher frequency contents can be easily calculated for far field source at an arbitrary site. By dividing a fault plane into small elements, this technique was applied to the synthesis of waves and the simulation of strong ground motions for near field source. The variability of this technique was shown and the fundamental data for synthesis and simulation on the strong ground motion were obtained.

The synthesis accelerogram of the respective waves that generate from small fault elements were calculated for two active faults that will affect severe damage on almost structures in the Osaka basin. It is found that the surface layer on a fault will affect the maximum acceleration of strong ground motions from the results of attenuation relationship between the maximum acceleration and the distance.

We need to get more detailed information on the soil structure and conditions and parameters of the source, and also discuss the simulation and the prediction of strong ground motions to examine the dynamic behavior of buildings and civil structures.

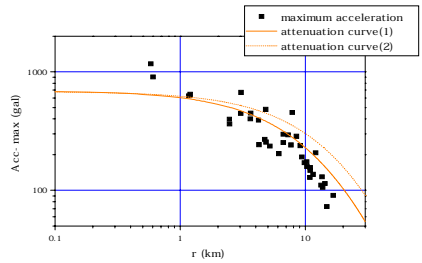

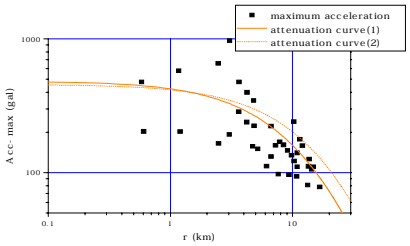

(a) d **=0.0, Uemachi fault** **(b)** d **=1.0 km, Uemachi fault**

Figure 11. Relation between the maximum acceleration values and the distance (r **).**

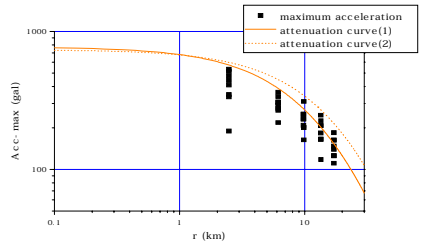

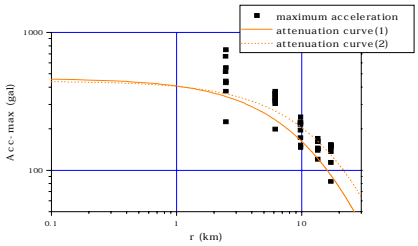

(c) d **=0.0, Ikoma fault** d **(d)=1.0 km, Ikoma faul**

Figure 12. Relation between the maximum acceleration values and the distance (r **).**

ACKNOWLEDGMENTS

The authors are grateful for the valuable suggestions of Dr. M. Horike, associate professor of Osaka Institute of Technology. We also thank Yonezawa K. and Suzuki T. for their help of calculations. This work was partially funded by the of Kansai University and Grant-in-Aid for Scientific Research (Nos. 09650642 and 1055200) of the Ministry of Education, Science and Culture.

REFERENCES

Aki, K. (1967), "Scaling law of seismic spectrum", *Jour. Geophys. Res.*, 72, pp1217-1231.

Aki, K. and Richards, G. P. (1980), *Quantitative seismology, Theory and methods*, San Francisco: Freeman and Company.

Boore, D. M. (1983), "Stochastic simulation of high frequency ground motions based on seismological models of the radiated spectra", *Bull. Seism. Soc. Am.*, 73, pp1865-1894.

Brune, J. N. (1970), "Tectonic stress and the spectra of seismic shear waves from earthquakes", *Jour. Geophys. Res.*, 75, pp4997-5009.

Fukushima, Y. and Midorikawa S. (1994), "Evaluation of site amplification factors based on average characteristics of frequency dependent Q^{-1} of sedimentary strata", *Trans. of AIJ*, 460, pp37-46 (in Japanese).

Irikura, K. (1986), "Prediction of strong acceleration motions using empirical Green function", *Proc. 7th Japan Earth. Symp*, pp151-156.

Irikura K. (1996), "Scenario earthquakes and strong ground motions for earthquake disaster prevention in Osaka and adjacent areas", Proc. 24 Symp. of Earthquake Ground Motion of AIJ, pp91-100 (in Japanese).

Kanamori, H. (1977). "The energy release in great earthquakes", *Jour. Geophys. Res.*, 82, pp2981-2987.

Kikuchi, M. (1995). "Teleseismic analysis of the Southern Hyogo (Kobe), Japan, earthquake of January 17, 1995", *Yokohama City Univ. Seismological note*, #38.

Lamb, E. H. (1904). "On the propagation of tremors over the surface of an elastic solid", Philosophical *Trans. of the Royal Society of London*, A203, pp1-42.

Somervill P. G., Irikura K., Sawada S., Iwasaki Y, Tai M. and Fushi M. (1993), "Spacial distribution of slip on earthquake faults", Proc. 22 JSCA Earthquake Engineering Symp., pp291-294 (in Japanese).

Trifunac, M. D. & Brady, A. G. (1975), "A study on the duration of strong earthquake ground motion", *Bull. Seism. Soc. Am.*, 65, pp581-626.

Utsu, T. (1982), "Relationship between earthquake magnitude scales", *Bull. Earth. Res. Inst.*, 57, pp465-497 (in Japanese).